Journal of Hazardous Materials 173 (2010) 563–569

Contents lists available at ScienceDirect

Journal of Hazardous Materials

journal homepage: www.elsevier.com/locate/jhazmat

Properties of sintered glass-ceramics prepared from plasma vitrified air pollution control residues

J.A. Roether[a], D.J. Daniel[a], D. Amutha Rani[a,b], D.E. Deegan[c], C.R. Cheeseman[b,**], A.R. Boccaccini[a,*]

[a] Department of Materials, Imperial College London, London SW7 2AZ, UK
[b] Department of Civil and Environmental Engineering, Imperial College London, London SW7 2AZ, UK
[c] Tetronics Ltd., Swindon, Wiltshire SN3 4DE, UK

ARTICLE INFO

Article history:
Received 25 March 2009
Received in revised form 24 August 2009
Accepted 26 August 2009
Available online 31 August 2009

Keywords:
Energy from waste
Air pollution control residues
Hazardous waste treatment
Plasma vitrification
Glass-ceramics

ABSTRACT

Air pollution control (APC) residues, obtained from a major UK energy from waste (EfW) plant, processing municipal solid waste, have been blended with silica and alumina and melted using DC plasma arc technology. The glass produced was crushed, milled, uni-axially pressed and sintered at temperatures between 750 and 1150 °C, and the glass-ceramics formed were investigated by X-ray diffraction (XRD), scanning electron microscopy (SEM) and transmission electron microscopy (TEM). Mechanical properties assessed included Vickers's hardness, flexural strength, Young's modulus and thermal shock resistance. The optimum sintering temperature was found to be 950 °C. This produced a glass-ceramic with high density (~2.58 g/cm^3), minimum water absorption (~2%) and relatively high mechanical strength (~81 ± 4 MPa). Thermal shock testing showed that 950 °C sintered samples could withstand a 700 °C quench in water without micro-cracking. The research demonstrates that glass-ceramics can be readily formed from DC plasma treated APC residues and that these have comparable properties to marble and porcelain. This novel approach represents a technically and commercially viable treatment option for APC residues that allow the beneficial reuse of this problematic waste.

1. Introduction

The aim of municipal solid waste (MSW) management should be to extract maximum value from this resource by maximising the recycling of valuable waste components [1]. There is a limit to what can be viably recycled, and combustion of the residual non-recyclable MSW in modern energy from waste (EfW) plants represents a safe and effective way of obtaining further value from MSW, both in terms of the energy generated, further extraction of metals and beneficial reuse of the incinerator bottom ash. National policy recognises EfW as a possible source of biomass energy and it is expected to have an increasing role in the waste management of industrialised countries such as the United Kingdom [2].

The release of atmospheric pollutants from EfW plants is controlled using air pollution abatement systems. These clean the air emissions to exceptionally high levels, but produce significant amounts of solid air pollution control (APC) residues [3,4]. These are classified as a hazardous waste, primarily because of their high alkalinity (pH > 12), although they also contain volatile heavy metals and organic contaminants, including dioxins and furans [5]. APC residues from EfW plants in some European countries are used to backfill salt mines, but this is not always a viable option. A number of treatments have been developed for APC residues ranging from physico-chemical treatment of acid wastes, solidification/stabilisation, vitrification and disposal in hazardous waste landfill [6–9].

Thermal processes at temperatures above 1400 °C produce inert glassy materials from silicate wastes that encapsulate heavy metals in a silicate network [10–14]. This process also considerably reduces the waste volume and produces a stable and inert glass, which is qualified for reuse as a product [15]. Thermal vitrification of incinerator bottom and fly ash with and without additions, e.g. glass cullet or feldspar, has successfully produced glass-ceramic products with adequate mechanical and physical properties [16–23].

Plasma technology has been used to treat incinerator fly ash [24–27], sludge from wastewater treatment [28] and other types of wastes [29]. The use of plasma technology to treat a variety of hazardous and non-hazardous waste has recently been reviewed [30].

APC residues of the type generated in the UK have been treated by DC plasma technology [15]. This produced a stable, inert glassy slag in which hazardous substances were immobilised and organic molecules effectively destroyed. APC residues do not contain

* Corresponding author. Tel.: +44 0207 5946731; fax: +44 0207 5946757.
** Corresponding author.
E-mail addresses: c.cheeseman@imperial.ac.uk (C.R. Cheeseman), a.boccaccini@imperial.ac.uk (A.R. Boccaccini).

0304-3894/$ – see front matter © 2009 Elsevier B.V. All rights reserved.
doi:10.1016/j.jhazmat.2009.08.123

sufficient glass-formers to produce a single-phase amorphous glass, and so silica and alumina were added. Leaching tests using the EU waste acceptance criteria (WAC) compliance leach tests demonstrated leaching of heavy metals and soluble salts significantly below the WAC limits for inert landfill, as reported elsewhere [15], even if different member states may have different threshold due to the manner in which they adopt and interpret the Landfill Directive.

There is potential for producing glass-ceramics from DC plasma treated APC residues using tailored heat-treatments [31]. Glass-ceramics have certain advantages over traditional polycrystalline ceramics as low porosity can be achieved at relatively low temperatures by exploiting viscous flow sintering [16,32]. They exhibit mechanical properties, chemical durability and thermal shock resistance superior to those of glass, and in some cases traditional ceramics [33].

The crystallisation of a glass to obtain a glass-ceramic is a heterogeneous transformation that involves nucleation and crystal growth. In the powder processing route glass powder is pressed into a compact that is sintered at high temperature. During heating the density of the compact increases due to viscous flow prior to crystallisation to form a glass-ceramic [34]. Glass-ceramics prepared by controlled crystallisation of wastes such as coal fly ash, wastes from hydrometallurgy and fly ash from municipal solid waste incineration have been reported [16,35,36].

Production of glass-ceramics by sintering and crystallisation of the glass produced by DC plasma treatment of APC residues has not previously been reported. The objective of this work was therefore to investigate the crystallisation process, sintered microstructure, mechanical properties and thermal shock resistance of the glass-ceramics formed.

2. Experimental

2.1. Processing of glass-ceramics

Glass produced by DC plasma treatment of APC residues was supplied as large sample blocks (typically 10 mm × 10 mm × 5 mm) by Tetronics Limited (Swindon, UK). The DC plasma furnace operates under controlled argon-rich conditions at temperatures of around 1600 °C and a detailed description of the process has been provided elsewhere [15]. Silica (T.J. Sansum, UK, 99% purity, <1 mm grain size) and alumina (added as Chinese bauxite, supplied by Ryder Point Processing, UK, 3–5 mm grain size) were added at 21.9 and 8.3 wt%, respectively, to the APC residues prior to plasma treatment. The addition of silica, as a glass former, and alumina, in order to increase the vitrification range of the system, has been proven to facilitate the conversion of APC residues to an inert glass by DC plasma treatment [15]. The chemical composition of the vitrified product is shown in Table 1.

Vitrified APC residue derived blocks were ground using a mill to obtain a powder with particle size <250 μm. An automatic pestle and mortar further reduced some of the <250 μm powder to a mean particle size of <75 μm. The resulting powders were uniaxially pressed using a steel die at 30 MPa to form 10 mm diameter, 4 mm high disc samples. No binders were added to the powders before pressing.

Based on preliminary differential thermal analysis (DTA) data, the pressed samples were heated at 10 °C/min from room temperature to sintering temperatures of 750, 850, 950, 1100 and 1150 °C and held at temperature for 2 h. In this case, it was assumed that surface nucleation will predominate leading to crystallisation during the holding time at temperature. The furnace was then cooled to around 200 °C at 10 °C/min when the samples were extracted and allowed to cool. Bar samples (40 mm × 4 mm × 3 mm) for use in mechanical property testing were also fabricated by uni-axial pressing at 30 MPa using a laboratory hydraulic press.

Table 1
Chemical composition of APC derived glass.

Oxides	Content (wt%)
Na_2O	0.15
MgO	1.39
Al_2O_3	14.64
SiO_2	40.87
P_2O_5	0.72
K_2O	<0.05
CaO	32.9
TiO_2	1.74
Mn_3O_4	0.21
V_2O_5	<0.05
Cr_2O_3	0.05
Fe_2O_3	4.57
BaO	0.05
ZrO_2	<0.05
ZnO	0.07
SrO	0.04
TC	0.01
S	0.07
Cl^-	2.6

2.2. Characterisation of sintered glass-ceramics

Scanning electron microscopy (SEM, Jeol JSM 840A) was used to examine the microstructure of polished, gold coated, glass-ceramic samples. Selected samples were etched in 10% HF and examined in secondary electron mode. Powdered samples were used for X-ray diffraction (XRD) analysis using a Philips PW 1825/00 diffractometer.

Specimens for transmission electron microscopy (TEM) observation were prepared from sintered materials using conventional mechanical polishing and ion beam thinning. The ion beam thinning was performed using a Gatan Model 691 Precision Ion Polishing System (PIPS). Bright-field (BF) images and calibrated selected-area electron diffraction (SAED) patterns were acquired using a JEOL JEM-2000EX TEM operating at 200 kV.

2.3. Physical properties

Sintered density was determined using Archimedes' method, with three specimens measured to calculate an average value using the following equation:

$$\text{density}\,(\text{g/cm}^3) = \frac{m_{dry}}{m_{sat} - m_{imm}} \times 100 \quad (1)$$

where m_{dry} is the dry mass, m_{imm} the immersed mass and m_{sat} the saturated surface-dry mass.

The percentage water absorption was calculated from m_{dry} and m_{sat} values using the equation:

$$\text{water absorption}\,(\%) = \frac{m_{sat} - m_{dry}}{m_{dry}} \times 100 \quad (2)$$

2.4. Mechanical property testing

Three-point bend strength values (Hounsfield H5KS tensile/compression testing machine) of five specimens for each sample type were obtained employing rectangular test bars using a 20 mm span. Young's modulus was determined by a non-destructive resonance frequency technique (Mk5 Grindosonic). The Vicker's hardness (HV) was determined using a Zwick/Roell Indetec ZHV instrument applying 500 g loads for 10 s. The average hardness was determined from six indents on polished surfaces.

2.5. Thermal shock testing

Thermal shock properties were determined by the water quench test [37]. This is the simplest method that provides a quantitative measure of the thermal shock resistance of ceramics and glass-ceramics. The critical quench temperature differential, ΔT_c and the residual strength level σ_r at $\Delta T < \Delta T_c$, were determined, where $\Delta T = T_{initial} - T_{water\ bath}$.

The thermal shock resistance test used cylindrical specimens (diameter $D = 7$ mm, thickness $t = 3$ mm). These were placed in a preheated furnace for 15 min before quenching into water at room temperature (volume = 1 l, $T_{water\ bath} = 20\,^{\circ}C$). Cyclic thermal shock tests for up to 10 cycles were also performed at $\Delta T = 500$ and $800\,^{\circ}C$.

Thermally shocked samples were tested for diametral compressive strength using a Zwick/Roell Z010 mechanical tester at a crosshead speed of 0.5 mm/min with the load applied until the onset of failure. Fig. 1 shows a schematic of the diametral compressive test. The diametral compressive strength σ_x was calculated using the following equation [38]:

$$\sigma_x = \frac{2P}{\pi D t} \tag{3}$$

where P is the applied force, t is the specimen thickness and D is the specimen diameter.

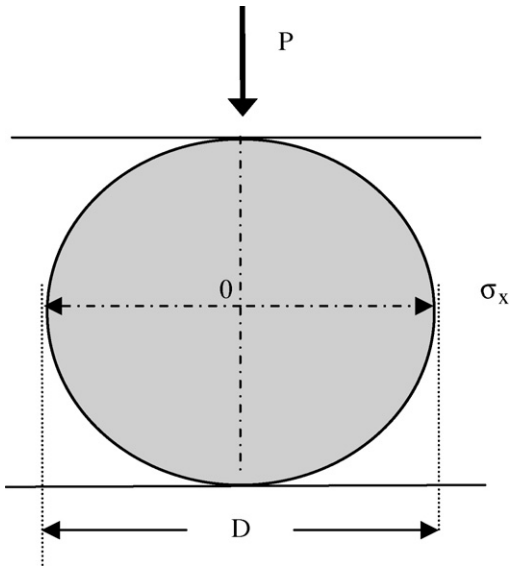

Fig. 1. Schematic diagram showing the disposition of a sample in the diametral compression strength test.

3. Results and discussion

3.1. Microstructural analysis

Sintered glass-ceramic samples showed a convenient sintering behaviour, i.e. the fired samples were homogeneous and free of defects such as large holes, bubbles or cracks. The SEM micrographs of glass-ceramics made from <75 μm powder are shown in Fig. 2. The image in Fig. 2a indicates that at 750 °C the grain boundaries are well defined and only partial sintering has occurred. At 850 °C (Fig. 2b) a higher degree of densification is evident, and the residual glass and new crystalline phases can be seen. At 950 °C (Fig. 2c) it is possible to identify a needle-like microstructure developing with increasing crystallisation. An interconnected needle-like morphology forms, while only a very small amount of residual glass remains. By 1100 °C (Fig. 2d), the needle-like structure can be observed and no residual glass is detected. It is also observed that the microstructure coarsened, which will have an impact on strength, as discussed below. Moreover, a small degree of porosity can be observed in the sintered samples.

Fig. 3(a–d) shows the microstructures of sintered samples made from plasma vitrified glass ground to <250 μm and sintered at different temperatures. Fig. 3a and b shows a well-developed

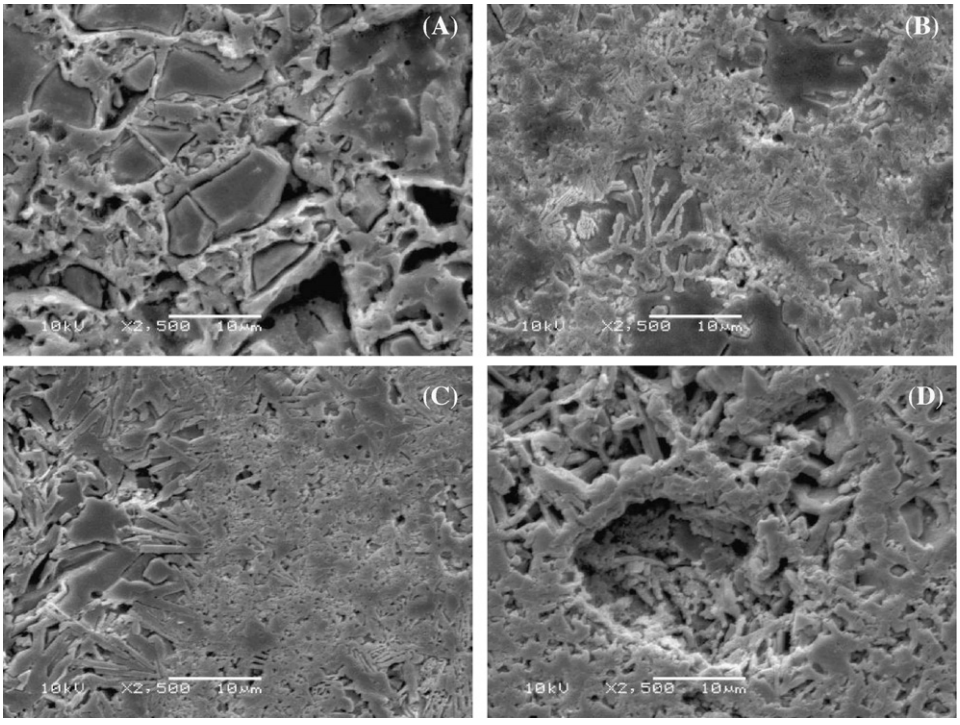

Fig. 2. SEM micrographs of sintered glass-ceramics fabricated from powders of particle size <75 μm at different temperatures: (A) 750 °C, (B) 850 °C, (C) 950 °C and (D) 1100 °C for 2 h. Samples were etched using 10% HF and examined in secondary electron mode.

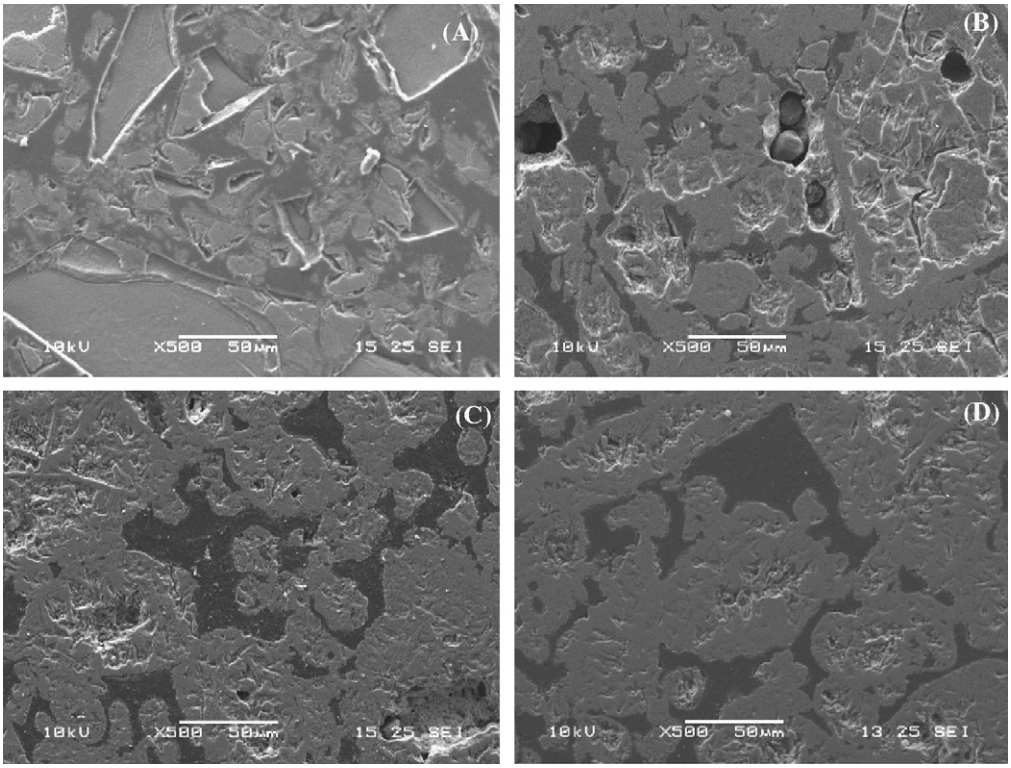

Fig. 3. SEM micrographs of sintered glass-ceramics fabricated from powders of particle size <250 μm at different temperatures: (A) 750 °C, (B) 850 °C, (C) 950 °C and (D) 1100 °C, for 2 h. Samples were etched using 10% HF and examined in secondary electron mode.

microstructure but the formation of new crystalline phases can be seen at high temperatures (Fig. 3c and d), and there is evidence of the needle-like crystals observed for samples sintered from <75 μm powder. However, whereas only a very small amount of glassy phase remained in samples sintered from the <75 μm glass powder, a much higher amount of glassy phase was observed in the <250 μm samples. The transformation from glass to glass-ceramic is seen to be enhanced in the material fabricated from glass powder with smaller particle size.

XRD analysis presented in Fig. 4 shows that at 750 °C the material is amorphous. Between 750 and 850 °C some crystalline phases appear, indicating the transformation from glass to glass-ceramic, and the intensity of the peaks increases with sintering temperature. Although this is not a quantitative analysis, an indication of the relative amounts of crystalline phases can be obtained by comparing the relative peak heights. Major phases observed were melilite $Ca_2(Mg_{0.5}Al_{0.5})(Si_{1.5}Al_{0.5}O_2)$ and wollastonite ($CaSiO_3$), with smaller amounts of anorthite ($CaAl_2Si_2O_8$) and kyanite (Al_2SiO_5) also detected.

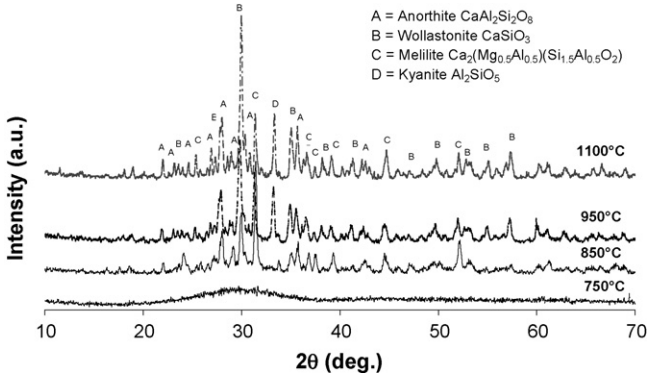

Fig. 4. XRD diffractograms of sintered discs made of powdered plasma vitrified APC residues at different temperatures (powder particle size <75 μm).

Fig. 5(a–e) shows the results of the TEM investigation (bright-field images and SAED patterns) on glass-ceramic samples made from <75 μm powder, sintered at 1100 °C for 2 h. It is observed from TEM micrographs (Fig. 5a and b) that many columnar grains are developed during the sintering process and that these elongated grains are within a glassy matrix. The SAED patterns were taken on these elongated grains and are shown in Fig. 5c and d. The SAED patterns can be indexed as β-wollastonite with 1*T* and 2 M polytypes, respectively. β-wollastonite was found as predominantly elongated (columnar) grains and this confirms the results obtained by SEM and XRD analyses. The TEM-BF image in Fig. 5e shows a triple junction and the corresponding SAED pattern shows the grain at the triple-point as a glassy phase. The TEM investigation shows that even after heat-treatment at 1100 °C, there is some residual glassy phase in the sample which could not be detected by XRD (Fig. 4).

3.2. Physical and mechanical properties

Fig. 6 shows the variation of density and water absorption with sintering temperature in glass-ceramics made from the powders with different particle sizes. Initially the green density was 2.49 g/cm^3. Density increases with heat-treatment up to a temperature of 950 °C when maximum densification occurs. Further increases in sintering temperature do not lead to increases in density.

The original glass powder apparent density was determined using helium pycnometry as 2.61 g/cm^3. The maximum sintered density at 950 °C was 2.60 g/cm^3 and therefore the relative density is around 95%. The lowest water absorption of the parent glass was ~2% compared to ~12% for the glass-ceramic sintered at 750 °C.

Table 2 shows the mechanical property data for these sintered glass-ceramics compared with other types of glass-ceramics and

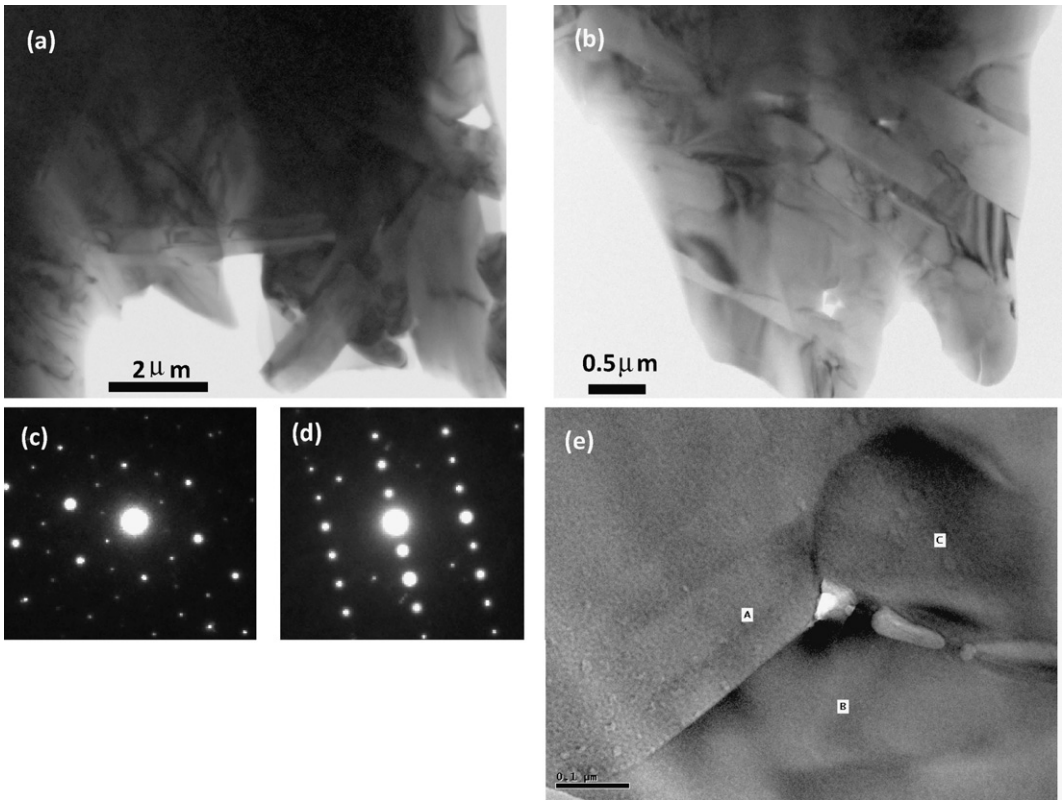

Fig. 5. TEM investigation of APC derived sintered glass-ceramic (particles size <75 μm): (a) TEM micrograph of glass-ceramic at 8k magnification, (b) TEM micrograph of glass-ceramic at 25k magnification, (c) diffraction pattern corresponding to (a) and (d) diffraction pattern corresponding to (b) and (e) TEM micrograph of the crystalline microstructure of the glass-ceramic at higher magnification.

Table 2
Comparison of mechanical properties, including density, Vickers hardness, Young's modulus, bending strength of APC residues derived glass, sintered glass-ceramics and other engineering materials from the literature.

Material property	APC residues derived glass	Sintered APC derived glass-ceramics	Granite [39,40]	Marble [39,40]	Porcelain stoneware tiles	Machineable glass-ceramics Corning Limited [45]
Density, g/cm^3	2.61	2.60	2.6–2.8	2.6–2.8	2.4	2.52
Vickers hardness, GPa	6.2 ± 0.2	6.0 ± 0.4	5.1–6.9	1.3–1.7	5.4–5.8 (44, 46)	2.3
Young's modulus, GPa	–	93 ± 5	43–61	28–84	58–70 (43, 46)	66.9
Bending strength, MPa	–	81 ± 4	12–15	14–17	78 (42, 46)	90

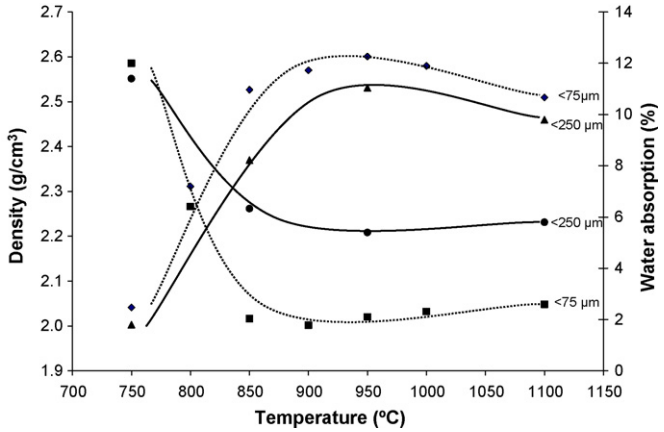

Fig. 6. Variation of density (in g/cm^3) and water absorption (in mass %) with sintering temperature for the compacted/sintered glass-ceramics from APC derived glass for two different particle sizes (♦ and ▲, density variation for glass-ceramics for particle sizes, 75 and 250 μm, respectively; ■ and ●, water absorption for particle sizes, 75 and 250 μm, respectively).

commercially available materials [39–44]. Natural stone tiles such as granite and marble have inferior mechanical properties and porcelains have comparable properties to the optimum glass-ceramic produced in this investigation. When comparing the mechanical properties of sintered glass-ceramics fabricated from APC derived glass to those of other glass-ceramics made from waste the APC derived glass-ceramics have equivalent or superior mechanical properties. For example, glass-ceramics made from incineration fly ash and glass cullet had comparable densities, but a Young's modulus of 85 GPa and bending strength of 60 MPa [39,40].

3.3. Thermal shock tests

Fig. 7 shows the diametral compressive strength (DCS) of glass-ceramics after 1 cycle of thermal shock. Up to $\Delta T = 750\,^{\circ}C$ no reduction in strength is observed. At $\Delta T = 800\,^{\circ}C$ the DCS is significantly reduced and this value of ΔT is considered to be the critical temperature difference leading to thermal shock fracture (ΔT_c). The residual strength of the sintered glass-ceramic material was found to be around 14 MPa. These results agree with previous work as the sample strength should show no changes for $\Delta T < \Delta T_c$,

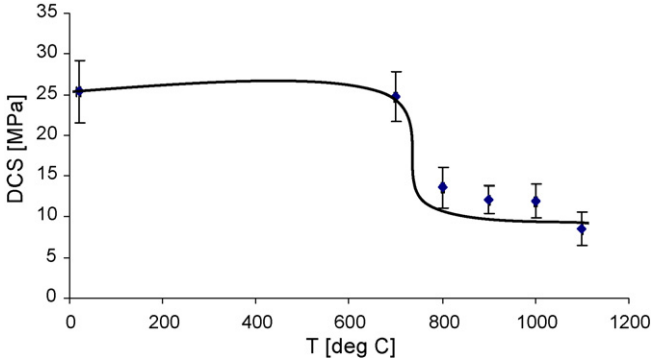

Fig. 7. Diametral compressive strength of sintered glass-ceramics (<250 μm) after one cycle of thermal shock using the water quench method at different temperatures up to 1100 °C. A sharp reduction in diametral tensile strength was noted around 750 °C. The line is added as help to the eye only, but the curve follows the expected shape of thermal shock resistance curves of brittle materials.

Table 3
Diametral compressive strength (DCS) in MPa of sintered glass-ceramics after thermal shock tests using the water quench method, i.e. after 1 cycle and after 10 cycles at ΔT = 500 and 800 °C.

Temperature (ΔT) in °C	DCS after 1 cycle, MPa	DCS after 10 cycles, MPa
500	25 (±4)	24 (±2)
800	14 (±2)	13 (±1)

No statistically significant reduction in DCS was observed after 10 cycles of thermal shock compared to 1 cycle of heating and quenching.

a rapid decline at $\Delta T = \Delta T_c$ and then negligible change for $\Delta T > \Delta T_c$ [37].

The thermal shock behaviour of the sintered glass-ceramics was determined for 10 cycles of heating and quenching at 500 and 800 °C. The results are shown in Table 3. No statistically significant reduction in diametral compressive strength was observed for either temperature.

The present results indicate that the glass-ceramics developed are attractive materials for high temperature applications (up to 750 °C) in oxidising environments. The favourable glass–crystal composite microstructure is thought to be responsible for this behaviour [33], considering that a much lower thermal shock resistance is expected for the amorphous parent glass.

4. Conclusions

Sintered glass-ceramics from plasma vitrified APC residue glass were produced by a pressureless powder sintering method. The mechanical properties investigated, including Vickers hardness, Young's modulus and bending strength were comparable to or superior to natural materials such as granite and marble, porcelain tiles, and commercially available glass-ceramics such as Macor™, and therefore these waste derived materials could find application in the construction sector. The mechanical properties of the glass-ceramics were also higher than those of similar glass-ceramics produced from other wastes, such as fly ash. The thermal shock resistance of the glass-ceramics made from plasma vitrified APC residue glass were high compared to other ceramic and glass materials, which implies potential for application as a refractory or as a matrix for high temperature composite materials. TEM results indicated that β-wollastonite exist as columnar grains within a crystalline matrix. A residual glassy phase is still present in the glass-ceramics even after firing at 1100 °C for 2 h. This dual glass-crystalline microstructure is responsible for the improved mechanical properties and thermal shock resistance of the sintered glass-ceramics.

Acknowledgements

This work was completed as part of the project 'Integrated solution for air pollution control residues (APCs) using DC plasma technology' funded by the UK Technology Strategy Board and Defra, through the Business Resource Efficiency and Waste (BREW) programme. The Technology Strategy Board is a business-led executive non-departmental public body, established by the government. Its mission is to promote and support research into, and development and exploitation of, technology and innovation for the benefit of UK business, in order to increase economic growth and improve the quality of life. It is sponsored by the Department for Innovation, Universities and Skills (DIUS) (visit www.innovateuk.org for further information). The authors would like to acknowledge the help of Miss Margaux Intilla and Miss Louisa Riera Lamela in the thermal shock experiments and diametral tensile strength testing.

References

[1] DEFRA Waste Strategy Annual Progress Report, 2007/08, Department for Environment, Food and Rural Affairs, July 2007.(http://www.defra.gov.uk/environment/waste/strategy/strategy07/pdf/waste-strategy-report-07-08.pdf).
[2] A.M. Ragossnig, C. Wartha, A. Kirchner, Energy efficiency in waste-to-energy and its relevance with regard to climate control, Waste Manage. Res. 26 (2008) 70–77.
[3] A. Porteous, Energy from waste: a wholly acceptable waste-management solution, Appl. Energy 58 (1997) 177–208.
[4] A. Porteous, Why energy from waste incineration is an essential component of environmentally responsible waste management, Waste Manage. 25 (2005) 451–459.
[5] T. Astrup, H. Mosbæk, T.H. Christensen, Assessment of long-term leaching from waste incineration air-pollution-control residues, Waste Manage. 26 (2006) 803–814.
[6] D. Geysen, C. Vandecasteele, M. Jaspers, G. Wauters, Comparison of immobilisation of air pollution control residues with cement and silica, J. Hazard. Mater. 128 (2006) 27–38.
[7] M. Fernandez Bertos, S.J.R. Simons, C.D. Hills, P.J. Carey, A review of accelerated carbonation technology in the treatment of cement-based materials and sequestration of CO_2, J. Hazard. Mater. 112 (2004) 193–205.
[8] K. Lundorp, D.L. Jensen, M.A. Sorensen, T.H. Christensen, E.P.B. Mogensen, Treatment of waste incincerator air-pollution-control residues with $FeSO_4$: concept and product characterisation, Waste Manage. Res. 20 (2002) 69–79.
[9] D. Amutha Rani, A.R. Boccaccini, D. Deegan, C.R. Cheeseman, Air pollution control residues from waste incineration: current UK situation and assessment of alternative technologies—review, Waste Manage. 28 (2008) 2279–2292.
[10] R. Cortez, H.H. Zaghloul, L.D. Stephenson, E.D. Smith, J.W. Wood, D.G. Cahill, Laboratory scale thermal plasma arc vitrification studies of heavy metal-laden waste, J. Air Waste Manage. 46 (1996) 1075–1080.
[11] M. Romero, R.D. Rawlings, J.Ma. Rincon, Crystal nucleation and growth in glasses from inorganic wastes from urban incineration, J. Non-Cryst. Solids 271 (2000) 106–118.
[12] P. Colombo, G. Brusatin, E. Bernardo, G. Scarinci, Inertization and reuse of waste materials by vitrification and fabrication of glass-based products, Curr. Opin. Solid State Mater. 7 (2003) 225–239.
[13] G. Palavit, E. Bekaert, G. Quoirin, L. Montagne, Vitrification of phosphated heavy metal waste in an alumino-silicate glass, Glass Sci. Technol. 77 (2004) 308–313.
[14] Y. Yang, Y. Xiao, J.H.L. Voncken, N. Wilson, Thermal treatment and vitrification of boiler ash from a municipal solid waste incinerator, J. Hazard. Mater. 154 (2008) 871–879.
[15] D. Amutha Rani, E. Gomez, A.R. Boccaccini, L. Hao, D. Deegan, C.R. Cheeseman, Plasma treatment of air pollution control residues, Waste Manage. 28 (2008) 1254–1262.
[16] A.R. Boccaccini, M. Petitmermet, E. Wintermantel, Glass-ceramics from municipal incinerator fly ash, Am. Ceram. Soc. Bull. 76 (1997) 75–78.
[17] Y. Park, J. Heo, Conversion to glass-ceramics from glasses made by MSW incinerator fly ash for recycling, Ceram. Int. 28 (2002) 689–694.
[18] Y. Park, J. Heo, Vitrification of fly ash from municipal solid waste incinerator, J. Hazard. Mater. B91 (2002) 83–93.
[19] F. Andreola, L. Barbieri, S. Hreglich, I. Lancellotti, L. Morselli, F. Passarini, I. Vassura, Reuse of incinerator bottom and fly ashes to obtain glassy materials, J. Hazard. Mater. 153 (2008) 1270–1274.
[20] M. Garcia-Valles, G. Avila, S. Martinez, R. Terradas, J.M. Nogues, Heavy metal-rich wastes sequester in mineral phases through a glass-ceramic process, Chemosphere 68 (2007) 1946–1953.
[21] C. Dimech, C.R. Cheeseman, S. Cook, J. Simon, A.R. Boccaccini, Production of sintered materials from air pollution control residues from waste incineration, J. Mater. Sci. 43 (2008) 4143–4151.

[22] M. Erol, S. Kucukbayrak, A. Ersoy-Mericboyu, Comparison of the properties of glass, glass-ceramic and ceramic materials produced from coal fly ash, J. Hazard. Mater. 153 (2008) 418–425.
[23] T.W. Cheng, M.Z. Huang, C.C. Tzeng, K.B. Cheng, T.H. Ueng, Production of coloured glass-ceramics from incinerator ash using thermal plasma technology, Chemosphere 68 (2007) 1937–1945.
[24] D. Deegan, C. Chapman, C. Bowen, The production of shaped glass-ceramic materials from inorganic waste precursors using controlled atmospheric DC plasma vitrification and crystallisation, High Temp. Mater. Proc. 7 (2003) 367–372.
[25] B.Y. Min, Y. Kang, P.S. Song, W.K. Choi, C.H. Jung, W.Z. Oh, Study on the vitrification of mixed radioactive waste by plasma arc melting, J. Ind. Eng. Chem. 13 (2007) 57–64.
[26] A.L. Mosse, A.V. Gorbunov, V.V. Sauchyn, Plasma furnaces for toxic waste processing, High Temp. Mater. Proc. 11 (2007) 205–217.
[27] J. Heberlein, A.B. Murphy, Thermal plasma waste treatment, J. Phys. D-Appl. Phys. 41 (2008) (Article No: 053001).
[28] H.I. Kim, D.W. Park, Characteristics of fly ash/sludge slags vitrified by thermal plasma, J. Ind. Eng. Chem. 10 (2004) 234–238.
[29] K. Katou, T. Asou, Y. Kurauchi, R. Sameshima, Melting municipal solid waste incineration residue by plasma melting furnace with a graphite electrode, Thin Solid Films 386 (2001) 183–188.
[30] E. Gomez, D. Amutha Rani, C.R. Cheeseman, D. Deegan, M. Wise, A.R. Boccaccini, Thermal plasma technology for the treatment of wastes: a critical review, J. Hazard. Mater. 161 (2009) 614–626.
[31] R.D. Rawlings, J.P. Wu, A.R. Boccaccini, Glass-ceramics:, Their production from wastes—a review, J. Mater. Sci. 41 (2006) 733–761.
[32] A.R. Boccaccini, W. Stumpfe, D.M.R. Taplin, C.B. Ponton, Densification and crystallisation of glass powder compacts during constant heating rate sintering, Mater. Sci. Eng. A 219 (1996) 26–31.
[33] P.W. MacMillan, Glass-ceramics, Second edition, Academic Press Inc., London, UK, 1979.
[34] J.M. Rincon, Principles of nucleation and controlled crystallization of glasses, Polym. -Plast. Technol. 31 (1992) 309–357.
[35] A.A. Francis, R.D. Rawlings, R. Sweeney, A.R. Boccaccini, Crystallization kinetic of glass particles prepared from a mixture of coal ash and soda-lime cullet glass, J. Non-Cryst. Solids 333 (2004) 187–193.
[36] J.M. Rincon, M. Romero, A.R. Boccaccini, Microstructural characterisation of a glass and a glass-ceramic obtained from municipal incinerator fly ash, J. Mater. Sci. 34 (1999) 4413–4423.
[37] D. Lewis III, Thermal shock and thermal shock fatigue testing of ceramics with the water quench test, in: Fracture Mechanics of Ceramics, Vol. 6: Measurements, Transformations, and High Temperature Fracture, Plenum Press, New York, 1983.
[38] M.K. Fahad, Stresses and failure in the diametral compression test, J. Mater. Sci. 31 (1996) 3723–3729.
[39] A. Karamanov, M. Pelino, A. Hreglich, Sintered glass-ceramics from municipal solid waste-incinerator fly ashes. Part I. The influence of the heating rate on the sinter-crystallisation, J. Eur. Ceram. Soc. 23 (2003) 827–832.
[40] A. Karamanov, M. Pelino, M. Salvo, I. Metekovits, Sintered glass-ceramics from incinerator fly ashes. Part II. The influence of the particle size and heat-treatment on the properties, J. Eur. Ceram. Soc. 23 (2003) 1609–1615.
[41] F. Andreola, L. Barbieri, E. Karamanova, I. Lancellotti, M. Pelino, Recycling of CRT panel glass as fluxing agent in the porcelain stoneware tile production, Ceram. Int. 34 (2008) 1289–1295.
[42] L. Esposito, A. Tucci, D. Naldi, The reliability of polished porcelain stoneware tiles, J. Eur. Ceram. Soc. 25 (2005) 1487–1498.
[43] J. Martín-Márquez, J.M. Rincón, M. Romero, Effect of firing temperature on sintering of porcelain stoneware tiles, Ceram. Int. 34 (2008) 1867–1873.
[44] L. Barbieri, L. Bonfatti, A.M. Ferrari, C. Leonelli, T. Manfredini, D. Settembre Blundo, Relationship between microstructure and mechanical properties in fully vitrified stoneware, in: P. Vincenzini (Ed.), Ceramics: Charting the Future, vol. 3A, Techna Srl, Modena, 1995, pp. 99–105.
[45] Corning product information: http://www.corning.com/docs/specialtymaterials/pisheets/Macor.pdf.